analytical chemistry

pubs.acs.org/ac Article

Viral Generation, Packaging, and Transduction on a Digital Microfluidic Platform

Angela B. V. Quach, Samuel R. Little, and Steve C. C. Shih*

Cite This: *Anal. Chem.* 2022, 94, 4039−4047 Read Online

ACCESS | Metrics & More | Article Recommendations | Supporting Information

ABSTRACT: Viral-based systems are a popular delivery method for introducing exogenous genetic material into mammalian cells. Unfortunately, the preparation of lentiviruses containing the machinery to edit the cells is labor-intensive, with steps requiring optimization and sensitive handling. To mitigate these challenges, we introduce the first microfluidic method that integrates lentiviral generation, packaging, and transduction. The new method allows the production of viral titers between 10^6 and 10^7 (similar to macroscale production) and high transduction efficiency for hard-to-transfect cell lines. We extend the technique for gene editing applications and show how this technique can be used to knock out and knock down estrogen receptor gene—a gene prominently responsible for 70% of breast cancer cases. This new technique is automated with multiplexing capabilities, which have the potential to standardize the methods for viral-based genome engineering.

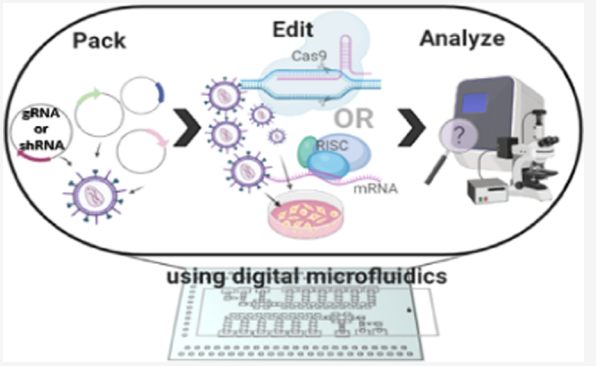

Virus-mediated gene editing is a widely used technique in which short-hairpin RNAs (shRNA)[1] or single-guide RNAs (sgRNA)[2] are packaged within viral particles and are delivered into the target cells. To prepare virus particles, co-transfection of three plasmids into a packaging cell line (e.g., HEK293T) is required to allow for the efficient production of viral particles that are released into the cells' supernatant. The viral particles (whether adeno- or lentiviral) can be harvested, purified, and titrated in preparation for infection. Using a viral-mediated approach leads to applications including editing cells for the treatment of genetic diseases[3,4] and in achieving highly specific immunotherapies[5−7] since viral delivery can integrate our gene of interest efficiently into the cells to create new designer antibodies or to gene-correct genetic deficiencies.

The most common method for preparing and producing viral vectors is to first seed a "packaging" cell line[8] in the presence of a nutrient-filled medium to form a monolayer culture. This is followed by preparing a co-transfection mixture (containing the packaging, envelope, and transfer plasmids), which is then added to the cells. This process requires that the reagent be added in a gentle dropwise manner such that there is no immediate change to the pH of the medium, allowing for the cells to maintain good health and to efficiently uptake the plasmids for production. The supernatant is harvested and pooled with several rounds of centrifugation and purification to improve vector potency and purity, making the overall process of preparing viral vectors tedious.[9] Once harvested, the titration of viral vectors must be performed to determine the concentration of the viral titers where different methods can be selected for measurement.[10] Aside from production, optimizing vector transduction to boost efficiency is another bottleneck—which depends on lengthy trial-and-error procedures to find the optimal viral parameters (i.e., viral concentrations, multiplicity of infection (MOI), transduction times) to achieve high efficiency. Working with standard transduction systems[11,12] requires large vector quantities, which calls for large working volumes (>100 μL), with much of the viral titer being wasted.

The challenges described above have driven much interest in miniaturizing lentiviral processes, especially transduction using a microfluidic device.[13−16] These approaches have been shown to reduce volumes for transduction, enable faster transduction rates, and overcome limitations that hinder efficient gene transfer. Owing to the increased surface-area-to-volume ratio at the miniaturized scale, these studies have shown fast lentiviral gene transfer kinetics and high transduction efficiency at lower volumes (~1 to 15 μL).[17] Thus, using microfluidics can be an enabling platform for lentiviral transduction. While these represent important steps forward, the methods do not integrate other important steps that are related to lentiviral transduction—generation and packaging—because they are limited in the complexities of cell cultivation of a packaging cell

Received: December 2, 2021
Accepted: January 25, 2022
Published: February 22, 2022

https://doi.org/10.1021/acs.analchem.1c05227
Anal. Chem. 2022, 94, 4039−4047

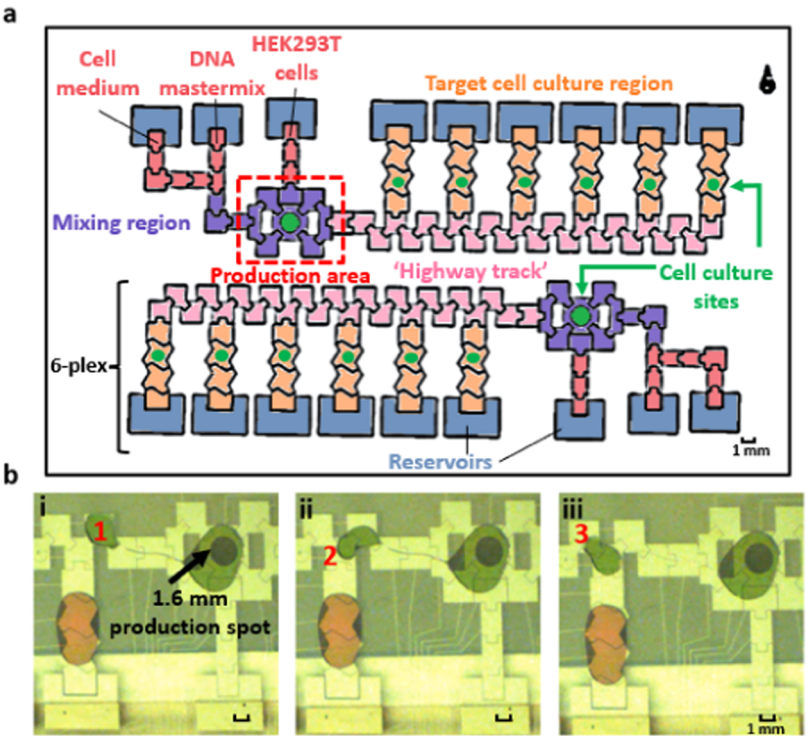

Figure 1. LENtiviral GENeration, packaging, transduction, and analysis (LENGEN) on a digital microfluidic platform. (a) Top-view schematic representation of the LENGEN device. The bottom plate contains two sets of 80 electrodes each for lentiviral generation and packaging, cell culturing, transduction, and analysis. For each set, there is one patterned 1.6 mm dia. cell culture site for production and six ∼1.2 mm dia. site for transduction and analysis. The production area houses a 3 μL droplet, which is split into unit droplets (∼1 μL) that covers the area of an electrode and actuated to the cell culturing sites. Two sets of electrodes enable replicates or different conditions to be performed in parallel. (b) Frames from a movie depicting (i) the droplet resting on electrode 1, (ii) droplet moves to electrode 2 when it is activated, and (iii) droplet shows unidirectional movement onto electrode 3 (and not electrode 1) when electrodes 1 and 3 are bussed. The "highway track" of electrodes is used to enable the delivery of the lentiviral particles to the cells with minimal electrode connections and to provide multiplexing capabilities on digital microfluidic devices. Droplets in the frames consisted of water, 0.05% Pluronics F-127, and food dye.

line, co-transfection of the plasmids, media and reagent exchange, and harvesting and purification of the viral particles for direct on-device functional titration. To address the challenges described above, we introduce a technique for expediting LENtiviral GENeration, packaging, production, and transduction (called LENGEN) on a digital-based microfluidic platform (DMF). There are many advantages in using DMF for automating such a process,[18] such as the ability to program all droplet operations and the ability to address each droplet individually. DMF is compatible for cell culturing, in which cells can be cultured in droplets,[19] on protein spots,[20] or on fabricated hydrophilic spots,[21−25] enabling automating processes like gene editing, which requires culturing cells over weeks. Finally, because the two-plate DMF system has a removable top substrate, cells cultured on this platform can be easily removed by trypsinization and transferred to another platform (e.g., well plate) for validation (reverse transcription polymerase chain reaction (RT-PCR), sequencing) and expansion.

Here, we describe a "proof-of-principle" method for viral generation, packaging, and transduction by DMF to perform automated site-specific gene editing and silencing. We demonstrate that our LENGEN device is effective for packaging lentiviral vectors up to 15 kb in size and producing lentiviral titers comparable to the gold-standard techniques. Furthermore, to extend the technique to be useful for gene editing/silencing, we integrated the transduction process on the same device to directly target the estrogen receptor in breast cancer cells using the produced lentiviral particles and performed validation/expansion of the edited cells. Using our platform, we reduce the time to package, produce lentiviruses and transduce target cells, analyze their edits while achieving the same results as in the macroscale, and reduce manual intervention (i.e., pipetting steps, purification and filtering, transferring of precious cells). To the best of our knowledge, this report is the first to describe a microfluidic technique that allows for lentiviral packaging, production, and transduction and we propose that the new techniques will be of value for automating procedures related to genome engineering applications.

EXPERIMENTAL SECTION

Microscale Cell Culture, Reverse Transfection, Viral Production, and Transduction. *Cell Culture.* Before seeding cells onto DMF devices, all cell types (H1299, HEK293T, MCF-7, MDA-MB-231, and T47D-KBLuc) used in this study were grown in 100 mm Petri dishes and were washed with PBS buffer, trypsinized with 0.25% trypsin−EDTA, and resuspended in complete medium (with 10% heat-inactivated fetal bovine serum (FBS)). After centrifugation, the cell pellet was resuspended in complete medium and cells were counted such that dilutions made would reach the required cell density. Aliquots of the cell suspension at densities (from ∼1.0 × 10^6 to 2.5 × 10^6 cells/mL) were supplemented with 0.05% w/v Pluronics F-127.

https://doi.org/10.1021/acs.analchem.1c05227
Anal. Chem. 2022, 94, 4039−4047

For cell seeding of the target cells, we followed a similar protocol as described previously.[21] Briefly, 1.5 μL of the above cell suspension was pipetted onto the bottom plate at the edge of the top plate and loaded by applying driving potentials (~500 V total, 15 kHz) into the appropriate reservoirs; 1.5 μL droplets were formed by elongating the liquid from the reservoir and activating the potential on an active dispensing electrode. The dispensed droplets from the reservoirs were actuated across a hydrophilic site (on the top plate) generating 1.5 and 1 μL volumes for eventual viral production and transduction, respectively. Excess liquid from the spot was actuated to a waste reservoir and removed with a KimWipe. Viral production steps were then done immediately after cell seeding.

Viral Production. HEK293T cells were seeded and cultured on the 1.6 mm diameter hydrophilic spot (following the cell culture protocol) at a suspension cell density of ~2.5×10^6–3.0×10^6 cells/mL. For viral production, we performed a reverse transfection protocol by first cotransfecting a mixture containing 0.75 μg of pMDLg/pRRE, 0.75 μg of pRSV-Rev, 1.5 μg of pMD2.g, and 3 μg of the transfer vector pLv-mCherry with 12.5 μL of lipofectamine 3000 and 12 μL of P3000 reagent for a total volume of 500 μL with Opti-MEM. After 20 min of incubation, 0.05% w/v of Pluronics F-127 was added to the mastermix to prepare for actuation on device; 1.5 μL of the lipofectamine mastermix was actively dispensed and actuated toward the seeded HEK293T cells. The formulation (3 μL total volume) was mixed in a circular fashion at the lentivirus production region by actuating adjacent electrodes (highlighted in the red box in Figure 1a).

Optimization of Viral Titers and Transduction. HEK293T cells were seeded and cultured at the "target cell" region at cell densities between 1 and 1.5×10^6 cells/mL following our cell culture protocol. After 24 h, four dilutions were generated containing the lentiviral particle-filled supernatant of the HEK293T cells at the production area. A dilution of 1:3 (Dulbecco's modified Eagle's medium (DMEM) and viral titers) was implemented by merging 1 μL of DMEM (10% heat-inactivated FBS, 8 μg/mL polybrene, 0.05% w/v Pluronics F-127; dispensed from the cell media reservoir) with 2 μL of the supernatant containing the viruses (Figure S1a). One microliter of the merged product was split and actuated to a "target cell" region, while the remainder (2 μL) was saved for other dilutions. This procedure was repeated three times to generate dilutions 1:6, 1:12, and 1:24. Two additional spots were used for controls where cells at the same density were cultured with a complete medium with 8 μg/mL polybrene on the first spot and without polybrene on the second spot. The device was flipped upside down and incubated overnight. After 24 and 48 h incubation, the device was imaged using an Olympus IX73 inverted microscope (Olympus Canada, Mississauga, ON, Canada) containing excitation and emission filters with wavelengths 585 nm and 608 nm, respectively, for mCherry fluorescence. We counted the fluorescent cells and estimated the viral titer using eq 1 (following Gill et al.[26])

$$\frac{\#\ \text{cells transduced} \times \%\ \text{fluorescent} \times \text{dilution factor}}{\text{transduction in volume}} = \text{transducing units per mL} = (\text{TU/mL}) \quad (1)$$

For CRISPR and shRNA optimization experiments, we followed the same procedures for cell culturing, viral production, and optimization of viral titers. The only changes to these procedures were the transfer plasmids were replaced with MISSION shRNA plasmids (i.e., TRCN00000003300, nontarget shRNA plasmid) and pLentiCRISPR-mCherry-NeoRv2 (LCMNv2) all-in-one Cas9 and sgRNA plasmids (Figure S1) for the shRNA and CRISPR experiments, respectively.

Expansion and Analysis. The next day, the transduced target cells were retrieved and pooled together with their corresponding dilutions 24 h post transduction. For example, 2 microwells that were subjected to the first serial dilution were pooled and 2 microwells that were subjected to the second serial dilution were pooled. The device was brought to a biological safety cabinet where the top plate was taken apart from the bottom plate. Five microliters of PBS was pipetted onto the microwells and aspirated using a Pasteur pipette, leaving only adhered cells on the microwell. Cells were detached using 2 μL of trypsin−EDTA (0.25% w/v), and the top plate was placed back in the humidifying chamber into the 37 °C with 5% CO_2 incubator for 2 min. Two microwells subjected to the same serial dilution from the same device were then pooled together by resuspending each microwell with 10 μL of complete medium and were added to 100 μL of complete media in a 96-well plate. The next day, the cultured wells were refreshed with complete medium supplemented with 1 μg/mL of puromycin for RNAi experiments and no antibiotics for CRISPR experiments. After 7 days post transduction, the cell lysate was collected for qRT-PCR assays or gene cleavage detection assays to verify gene knockouts.

RESULTS AND DISCUSSION

Lentiviral Generation (LENGEN): Digital Microfluidics for Viral Production and Transduction. Figure 1a shows a device to automate the production and the transduction of viral-derived vectors. Several design iterations were required to develop a device that is capable of producing and transducing virus particles. Two challenges were encountered in the process, including (1) generating the highest lentiviral titers that will enable efficient transduction and (2) performing a 12-plex viral transduction analysis on-chip. These challenges called for several innovations with the device design. First, to package and to produce lentiviruses, a host is required (e.g., HEK293T cells) that is easily transfected and supports a high level of expression of the viral proteins to allow for the efficient production of lentiviral titers. To enable such a process, we fabricated hydrophilic sites that are patterned on the device top plate to serve as sites for cell seeding and proliferation. These hydrophilic sites enable a procedure known as "passive dispensing" where a droplet is actuated across the site, and a small volume (~1.5 μL) of the droplet adheres to the site, seeding it with media and cells. Although cells have been cultured on hydrophilic spots previously,[21−25] this is the first time that is being used for continuous cultures to generate, produce, and deliver lentiviral particles. In initial experiments, we used a previous device design that cultured cells on ~1.2 mm diameter hydrophilic sites that enabled lipofection-mediated transfection with high efficiency.[21] However, using this device, we observed that (1) the production of the lentiviral titers generated very low or near 0% transduction efficiency and (2) the electrode configuration made it difficult to mix droplets containing the DNA and lipids resulting in

https://doi.org/10.1021/acs.analchem.1c05227
Anal. Chem. 2022, 94, 4039−4047

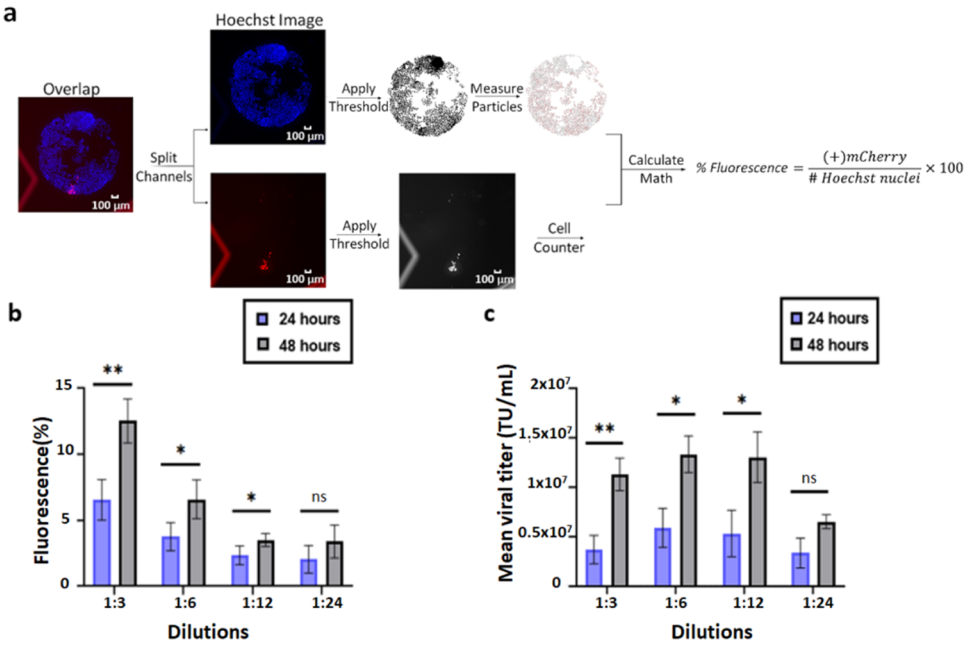

Figure 2. Optimizing lentiviral production. Schematic (a) showing the imaging pipeline used to measure the fluorescence of mCherry-positive cells. Plots show the (b) fluorescence efficiency and (c) mean viral titer as a function of supernatant dilutions (1:3, 1:6, 1:12, and 1:24) for positive mCherry HEK293T cells after 24 and 48 h lentiviral production and transduction. For panel (a), the schematic shows the workflow to calculate the % fluorescence (of mCherry) after viral transduction. Mean viral titer can then be calculated using eq 1. For panel (b), positive mCherry cells were counted and divided by nontransduced mCherry cells. For panel (c), the estimated mean viral titer amount was calculated by multiplying the number of cells transduced with the percentage of fluorescence, dilution factor, and dividing the total by the volume of lentiviral particles used for transduction (i.e., transducing units (TUs) per milliliter). Student's *t* test ($P < 0.05$) was used to evaluate the significance (* for a $P \leq 0.05$, ** for a $P \leq 0.01$, and ns for $P > 0.05$) between the dilutions. Error bars for both plots represent ±1 SD with N = triplicates.

uneven distribution of viral particles when harvesting the virus from the generation site. We hypothesize that the low transduction efficiency is due to the low viral titers being generated from the low cell density (~700 cells). Therefore, we created a larger cell culture site (~1.6 mm dia.) that houses ~2500 cells at the optimal 50−70% confluency. Although increasing the cell culture site can generate more viral titers and increase transduction efficiency, droplet movement away from the hydrophilic culture site can be challenging.[22] This is especially problematic if we are to generate a dilution series, which requires droplet movement away from the generation/packaging site and then mix/merge with dilution buffer. Hence, with a larger diameter (1.6 mm), a balance is struck between the lentiviral generation and the droplet movement forces to ensure we can generate dilutions, obtain high transduction efficiency, and continue to maintain reliable droplet movement.

In addition, we created a four-prong electrode system (highlighted as the "production area") that is directed toward the hydrophilic site. The latter innovation was particularly important for reliable droplet mixing and splitting since the droplet is continuously circulated around the four-prong electrode to facilitate uniform mixing and is easily extended to facilitate "necking" during droplet splitting. To fulfill the 12-plex capabilities, the device design contains a "highway track" to enable one-directional movement toward the cell culturing site and the delivery of the lentiviral particles to six target sites. Generally, square or interdigitated electrodes are used to facilitate droplet operations on a digital microfluidic device;[21,27,28] however, these types of electrodes require complicated wiring schemes that can be difficult to design as we increase the electrode density (unless you use multilayer fabrication techniques[29]). Instead, we modified the electrode design such that the droplet only moves toward the overlapping "prong" electrodes (Figure 1b). Using such a design allows the electrodes to be bussed through a minimal two connections—i.e., on our device design, we connected 22 electrodes using only 2 wired connections (instead of 22 wired connections)—saving time during the design phase. Moreover, the reduction in connections enabled us to incorporate a symmetrical design on the device to allow 12-plex transduction assays to be conducted simultaneously—replicating the 6-plex design on the same substrate. We anticipate that future designs can use such electrode designs to overcome multiplexing challenges that are commonly associated with digital microfluidics.

With this configuration, a five-step procedure was developed to facilitate the automated generation, packaging, and delivery of the virus system. The schematic shows the events at the genetic level with an image-based representation of the droplet movements on the device. As shown in Figure S2, in step (i), the producer cells (HEK293T) are in a droplet suspension and actuated to the production area by loading and dispensing from reservoirs. In step (ii), a unit droplet of liposomes and viral DNA plasmids (pMDLg/pRRE, pRev, pMD2.G, and transfer plasmid (Figure S3)) are dispensed and merged and are thoroughly mixed using a four-electrode linear array (~1 min for mixing). The lipofectamine mixture was incubated at room temperature for ~15−20 min for the DNA−liposomal complexes to be formed. In steps (iii−iv), the lipofectamine mixture was actuated to the HEK293T cells and actively mixed for 1 min via three continuous circulations in the production area containing eight electrodes to replicate the reverse transfection procedure on the device (i.e., adding transfection

https://doi.org/10.1021/acs.analchem.1c05227
Anal. Chem. 2022, 94, 4039−4047

mixture to unseeded cells). Finally, in step (v), after 24 h, the lentiviral particles were produced in the supernatant (cells are adhered to the hydrophilic spot) and specific dilutions (1:3, 1:6, 1:12, and 1:24) are formed via electrode actuation (with ~98% accuracy[28]) to infect target cells following the step-by-step procedure shown in the Supporting Information Figure S1a. The five-step droplet operation procedures are performed in ~5 min (see the Supporting Video) with several incubation periods (step ii: ~20 min; step v: overnight). This is the first (to the best of our knowledge) that is capable of automating the procedures of preparation, production, and transduction with viral-derived vectors at a faster rate than the macroscale techniques.[13]

Breast cancer cell lines (MCF-7 and T47DKB-Luc) were chosen as models for our lentiviral study to show that our automated platform can genetically modify oncogenes and use this method to potentially find therapeutic targets against these genes.[30] For all results described here, a droplet comprised of the breast cancer cells (at various cell densities) was loaded into the reservoirs. These droplets were dispensed into smaller volumes and actuated toward the cell culturing sites using passive dispensing techniques (as described above). Two parameters were evaluated: cell viability and transduction efficiency. As described in the Supporting Information (Figure S4), both cell lines were viable on the device and showed comparable viability when cultured in well plates. We also evaluated the cell viability after 48 and 72 h (since the gene knockouts after lentiviral transduction occur within this time frame[31,32]), and we observed an average viability of 83.7 and 85.7% for MCF-7 and 98.4 and 88.6% for T47DKB-Luc on the device. Figure S5a shows representative fluorescently labeled images of the MCF-7 and T47DKB-Luc cells, and as shown, the cells are proliferative, and the morphologies of the cultured breast cancer cells were similar to the cells cultured in well plates (Figure S4c,d). An additional assay was developed to determine if transduction can be performed (after generation and packaging) on device, and as shown in Figure S5b, the efficiency is ~43.0% after 48 h post transduction and improves to ~60.1% after 96 h post transduction for T47DKB-Luc cells. These efficiencies are also a significant improvement from lipid-based transfection (see Figure S6), which is a trend usually observed for hard-to-transfect cell lines like T47DKB-Luc.[33]

From the literature, a critical factor to determine successful lentiviral transduction is the functional titer, which is the transduction unit of a virus capable of infecting cells and expressing the transgene.[34,35] Hence, we performed four serial dilutions of the lentiviral particles containing a nontargeting plasmid mCherry to determine the optimal concentration of functional lentiviral obtained in HEK293T cells. A number of mCherry-transduced cells were counted (using imaging techniques, see Figure 2a) on the hydrophilic spot after 24 h and 48 h (Figure 2b). As shown, the most optimal concentration of lentiviral particles was observed after 48 h transduction—achieving a range of 6.5×10^6–1.33×10^7 TU/mL with the 1:3 dilution. These values were also translated to a viral titer (using eq 1 from the Experimental Section), and on-device, we were able to obtain a functional titer of $\sim 1 \times 10^7$ TU/mL after 24 or 48 h (Figure 2c)—values very similar to titers obtained from benchtop methods.[36,37]

Furthermore, we calculated the amount of transducing units generated per cell on the device and compared it to the macroscale techniques. On average, we produced 1.56 and 2.65 TU/cell on device after 24 and 48 h, respectively, which is very similar to the benchtop after 5 days of harvesting (~2.80 TU/cell) (Table 1; see Figure S7 for sample calculations). The fast production of titers and droplet manipulations (and larger surface-area-to-volume ratio) enables the drastic time reduction (approximately 2 weeks[32,38] to ~2 days; Figure S12) in packaging, producing, and transducing on device. In practice, it was decided that 24 h post-transduction step was sufficient for the gene silencing and editing assays given the titers generated at 24 h are sufficient for observing knockdown and knockout events (see below).

Table 1. Comparison of Lentiviral Production on LENGEN vs Macroscale

microscale (24 h)		microscale (48 h)		macroscale (5 days)	
dilutions	TU/cell*	dilutions	TU/cell	dilution	TU/cell
1:03	1.23	1:03	3.55	3:10	2.81
1:06	1.92	1:06	2.60	2:10	2.73
1:12	1.77	1:12	2.30	1:10	1.95
1:24	1.33	1:24	2.13	0.5:10	3.73
average	1.56	average	2.65	average	2.80

*TU/cell = transducing units per cell.

Other factors that affect the transduction efficiency are the size of the lentiviral payload[39,40] and cell type.[41] Since shRNA and CRISPR vectors are usually ~7.0 to 15.0 kb in size (compared to smaller ~4 kb plasmids containing fluorescent reporter mCherry), we used the system above to evaluate the effects of the lentiviral payload of ~15.0 kb (using LCMNv2—see Figure S3) in hard-to-transfect cell lines like H1299 and T47DKb-Luc. As shown in Supporting Figure S8a, we obtained the highest efficiency for the 1:3 dilution, which correspond to ~10.8% of H1299 cells that show mCherry fluorescence. Comparatively to H1299, T47DKb-Luc shows higher transduction efficiency with the 1:6 dilution at ~5% (Figure S8b), which is expected given that different cell lines have different affinities for virus uptake.[42,43] It is generally observed that larger lentiviral payloads will lead to lower transduction efficiency,[44] but there is no clear mechanism to predict which cell line will transduce more efficiently.[45] However, the results do suggest that for a particular cell type there should be a focus on optimizing MOIs or lentiviral dilutions and post-infection incubation times to obtain effective transduction. In the future, it may be important to further study different strategies[46,47] for effective transduction of lentiviral particles, especially if the application calls for a wide variety of cell types (immortalized, primary, stem, etc.).

LENGEN for Lentiviral Knockdown and Knockout Assays. To evaluate the potential of our system for knockdown and knockout assays, we packaged shRNA and CRISPR plasmids that will target the estrogen receptor α (ESR1) in breast cancer cells using our LENGEN system and then isolating single clones for expansion. ESR1 controls a wide range of physiological and regulatory processes in the development of the female reproductive system and is expressed in approximately 70% of breast cancer tumors.[48] Thus, there is much interest in systematically investigating genes whose loss affects cell growth or increases the estrogen-independent growth of ER+ breast cancer cells.[49] In this part of the work, we applied our system to automate the process of generating, packaging, and transducing the lentiviral particles

https://doi.org/10.1021/acs.analchem.1c05227
Anal. Chem. 2022, 94, 4039−4047

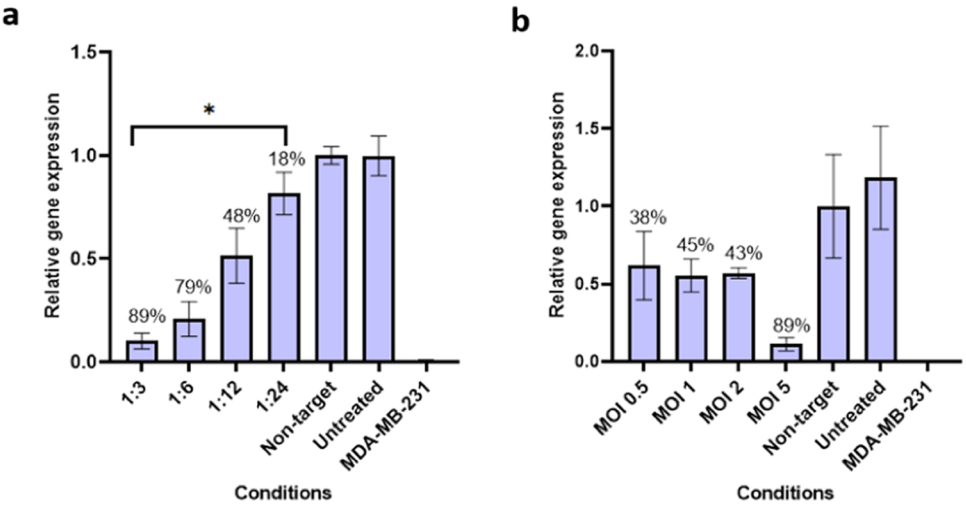

Figure 3. shRNA knockdown assays for ESR1. Evaluating the relative gene expression of estrogen receptor 1 (ESR1) in MCF-7 cells that were performed in (a) LENGEN device and (b) well plates. We generated, packaged lentiviral particles containing shRNAs targeting ESR1, and transduced them in MCF-7 cells. shRNA-mediated silencing of ESR1 was assessed using a ΔΔCq method to determine the relative gene expression from qRT-PCR data with ACTB (β-actin) as an endogenous reference gene. The cells exhibited MOI-dependent viral delivery of the shRNA targeting ESR1 knockdown, with mRNA transcript reduction by 38, 45, 43, and 89% when cells were treated with an MOI of 0.5, 1, 2, and 5, respectively. In the case with LENGEN, the cells exhibited dilution-dependent viral delivery of the shRNA targeting ESR1 knockdown, with mRNA transcript reduction by 89%, 79%, 48%, and 18% when cells were treated with dilutions 1:3, 1:6, 1:12, and 1:24, respectively. Significance between dilutions 1:3 and 1:24 is significant (shown as * for $P \leq 0.05$). Comparison of nontargeting shRNA (not targeting any known genes in any species) to untreated samples shows no significant effect on gene expression. A negative control depicts ESR1's relative downregulated expression (almost zero expression levels) in MDA-MB-231 cells. Error bars for both plots represent ±1 SD with N = triplicate.

containing the ESR1 target and examining the knockdown (shRNA) or knockout (CRISPR-Cas9) of the target gene.

To test the effectiveness of our method for gene expression analysis, RNAi assays were performed on the LENGEN device. The transfer plasmid targeting the ESR1 is packaged and produced using HEK293T cells, and the supernatant is diluted to different viral concentrations using DMF actuation (1:3, 1:6, 1:12, and 1:24; see Figure S1a), which are used to transduce MCF-7 cells. Expression values from LENGEN protocols were obtained by qRT-PCR methods by removing the top plate containing the transduced cells from the DMF device (via trypsinization) and transferring "pooled" cells (~2800 cells) to well plates for analysis after outgrowth for 7 days. For higher dilution (1:24) and lower dilution concentrations (1:3), the relative reduction in gene knockdown is 18 ± 8.8 % and 89 ± 37.6 %, respectively (Figure 3a), and is very similar to the observed in lentiviral well-plate conditions (Figure 3b). The gene expression percentages for both LENGEN and standard conditions were confirmed by a ΔΔCq method[50] (values obtained from Figure S9—qPCR amplification curves), which show that the LENGEN method is capable of gene silencing using viral delivery.

The knockout assay was motivated by the widespread interest in using CRISPR for identifying essential genes related to cancer and other diseases.[51−53] Similar to the RNAi assays, MCF-7 cells were seeded, grown, and transduced by a dilution series (generated on-chip) of lentiviruses containing an all-in-one plasmid with the Cas9 gene cassette and an sgRNA guide targeting ESR1. As shown in Figure 4a, the trend is very similar to what is observed with the RNAi experiments—i.e., at 1:3 dilution, we observed more cells being transduced—and this trend was identical to that observed in standard conditions (Figure 4b) and in the literature.[54] To verify the knockout, we performed downstream analysis by removing the MCF-7 cells (~2800 cells) from the device and culturing them in well plates in preparation for a genomic cleavage assay (Figure 4c). The band patterns and their cleavage percentages are similar to what is observed in the genomic cleavage gel from MCF-7 cells transduced (and lentiviral generation and packaging) in well plates at different MOIs (Figure 4d). Since genome editing efficiency varies with different cell lines,[55] we implemented the gene editing workflow[56] on H1299 cells and similarly observed the successful knockout of integrated eGFP (gene cleavage efficiency of 16.1%) (Figure S10). Although downstream gene editing analysis of CRISPR knockouts from microfluidic devices has been shown previously,[57−60] this is the first demonstration showing the integration of lentiviral packaging, generation, and transduction on a microfluidic device followed by downstream gene editing analysis (single clone isolation and expansion).

As depicted in Figure 1, this "proof-of-principle" method was carried out in a 12-plex format (through the use of "highway tracks"), and we propose that this will be straightforward to expand this technique to much higher levels of multiplexing given the electrode and bussing techniques presented here (and particularly with recent reports of active matrix methods[29,61]). We constructed lentiviral plasmids (Figure S11; available on Addgene) to perform lentiviral packaging, production, and transduction for knockdown (RNAi) and knockout (CRISPR) assays and we obtained very similar gene expression profiles compared to benchtop assays, with shorter time scales (days vs weeks) to obtain viral titers at sufficient levels, 100-fold savings in volumes to save precious lentiviral samples, and using minimal number of cells (~1000 to 3000 cells). In addition, in the macroscale, generating very concentrated amounts of viral titer requires several days of lentiviral harvests within large batches of culture and rounds of ultracentrifugation—a process that is not required with LENGEN techniques. Although this device generates a low number of transduced cells (i.e., ~1400 cells per target spot),

https://doi.org/10.1021/acs.analchem.1c05227
Anal. Chem. 2022, 94, 4039−4047

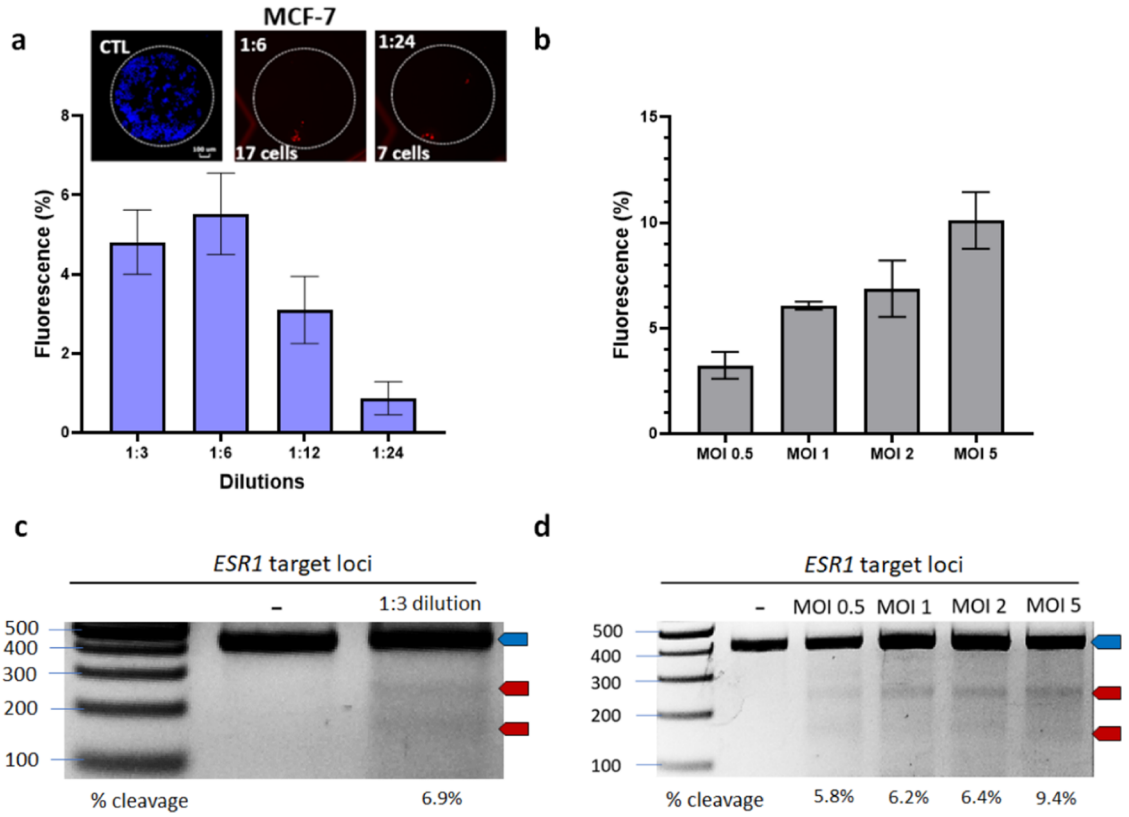

Figure 4. Knockout assays for ESR1. Evaluating the knockout efficiency of ESR1 in MCF-7 cells performed in well plates and on LENGEN. Lentiviral particles containing all-in-one Cas9/sgRNA targeting ESR1 were generated, packaged, and transduced using (a) LENGEN or (b) well-plate protocols. Plots of mCherry fluorescence (% of positive cells) were measured at (a) different dilutions (1:3, 1:6, 1:12, 1:24) and (b) different MOIs (0.5, 1, 2, and 5) by staining wild-type MCF-7 cells with Hoechst 33342 and compared to transduced (+)mCherry cells. (c, d) Each transduction was verified by a genomic cleavage assay after 7 days post transduction. The parental band is 409 bp (shown by the blue arrow), and the cleavage bands are 235 and 174 bp (shown by red arrows). Following LENGEN protocols, cells were removed from the top plate, transferred to a well plate, and the 1:3 transduced cells were pooled together to perform the genomic cleavage assay. Error bars for both plots represent ±1 SD with N = triplicate.

we believe a future generation of this platform will allow for more transduced cells via "pooling" of target cells by increasing the target spot area or increasing the droplet volumes in the production area to mL range. Therefore, our current platform is aimed to reduce the time for lentiviral packaging, production, and transduction of target cells, which has substantially decreased from generally 2 weeks[32,38] to 2 days (Figure S12), and to eliminate the tedium needed for packaging and producing (and transducing) lentiviruses.

CONCLUSIONS

In summary, we report the first demonstration of lentiviral generation packaging, production, and transduction for gene disruption using a digital microfluidic platform, with an application to target the estrogen receptor α gene in breast cancer cells. The new method incorporates a novel electrode design, enabling the optimal generation of lentiviral titers and multiplexing of viral transduction analysis on-device. We characterized the integration of lentiviral generation and production on DMF, which showed similar performance as the gold-standard techniques. Since our platform is automated, we applied LENGEN to gene disruption (RNAi) or editing (CRISPR-Cas9) assays, which showed excellent knockdown and knockout efficiencies, respectively. We anticipate that this new method will be useful for researchers seeking to greatly speed up (days instead of weeks) lentiviral production and transduction processes and to alleviate the tedium associated with optimizing lentiviral generation and transduction.

ASSOCIATED CONTENT

Supporting Information

The Supporting Information is available free of charge at https://pubs.acs.org/doi/10.1021/acs.analchem.1c05227.

Additional experimental details (reagents and materials, device fabrication, plasmid construction, automation setup, cell culture, qRT-PCR, gene cleavage assays, imaging pipeline using Image J), including figures showing additional data from transduction, knockdown, and knockout experiments, and tables containing primers and target sequences used in this study (PDF)

Food dyes to depict lentiviral workflow performed on device (MOV)

AUTHOR INFORMATION

Corresponding Author

Steve C. C. Shih − *Department of Biology, Concordia University, Montréal, Québec H4B 1R6, Canada; Centre for Applied Synthetic Biology, Concordia University, Montréal, Québec H4B 1R6, Canada; Department of Electrical and Computer Engineering, Concordia University, Montréal, Québec H3G 1M8, Canada;* orcid.org/0000-0003-3540-

https://doi.org/10.1021/acs.analchem.1c05227
Anal. Chem. 2022, 94, 4039−4047

0808; Phone: +1-(514) 848-2424; Email: steve.shih@concordia.ca

Authors

Angela B. V. Quach − *Department of Biology, Concordia University, Montréal, Québec H4B 1R6, Canada; Centre for Applied Synthetic Biology, Concordia University, Montréal, Québec H4B 1R6, Canada*

Samuel R. Little − *Centre for Applied Synthetic Biology, Concordia University, Montréal, Québec H4B 1R6, Canada; Department of Electrical and Computer Engineering, Concordia University, Montréal, Québec H3G 1M8, Canada*

Complete contact information is available at: https://pubs.acs.org/10.1021/acs.analchem.1c05227

Author Contributions

The research was designed by A.B.V.Q and S.C.C.S. All experiments and analysis were conducted by A.B.V.Q. and S.C.C.S. Biological and microfluidic methods were developed by A.B.V.Q. and S.R.L. All authors wrote, revised, and reviewed the manuscript.

Notes

The authors declare no competing financial interest.

■ ACKNOWLEDGMENTS

The authors would like to thank Dr. Sylvie Mader and her former student Dr. Justyna Kulpa for fruitful discussions on lentiviral packaging and transduction, Dr. Chris Law for microscope training at the Center for Microscopy and Cellular Imaging (CMCI), Dr. David Walsh for access to the PCR system, Hugo Sinha (DropGenie) and Kevin Larocque (Dr. Alisa Piekny lab) for cell culture and gene editing advice. For funding, we like to thank the Natural Sciences and Engineering Research Council (NSERC) (including the SynBioApps CREATE program), the Fonds de Recherche Nature et Technologies (FRQNT), MEDTEQ+, and the Canadian Foundation of Innovation (CFI). S.R.L. thanks NSERC for CGS M and D scholarships and the Concordia University Department of Electrical and Computer Engineering for FRS Funding. S.C.C.S. thanks Concordia for a University Research Chair.

■ REFERENCES

(1) Simpson, K. J.; Selfors, L. M.; Bui, J.; Reynolds, A.; Leake, D.; Khvorova, A.; Brugge, J. S. *Nat. Cell Biol.* **2008**, *10*, 1027−1038.
(2) Shalem, O.; Sanjana, N. E.; Hartenian, E.; Shi, X.; Scott, D. A.; Mikkelsen, T. S.; Heckl, D.; Ebert, B. L.; Root, D. E.; Doench, J. G.; Zhang, F. *Science* **2014**, *343*, 84−87.
(3) Aiuti, A.; Biasco, L.; Scaramuzza, S.; Ferrua, F.; Cicalese, M. P.; Baricordi, C.; Dionisio, F.; Calabria, A.; Giannelli, S.; Castiello, M. C.; Bosticardo, M.; Evangelio, C.; Assanelli, A.; Casiraghi, M.; Di Nunzio, S.; Callegaro, L.; Benati, C.; Rizzardi, P.; Pellin, D.; Di Serio, C.; Schmidt, M.; Von Kalle, C.; Gardner, J.; Mehta, N.; Neduva, V.; Dow, D. J.; Galy, A.; Miniero, R.; Finocchi, A.; Metin, A.; Banerjee, P. P.; Orange, J. S.; Galimberti, S.; Valsecchi, M. G.; Biffi, A.; Montini, E.; Villa, A.; Ciceri, F.; Roncarolo, M. G.; Naldini, L. *Science* **2013**, *341*, No. 1233151.
(4) McGarrity, G. J.; Hoyah, G.; Winemiller, A.; Andre, K.; Stein, D.; Blick, G.; Greenberg, R. N.; Kinder, C.; Zolopa, A.; Binder-Scholl, G.; Tebas, P.; June, C. H.; Humeau, L. M.; Rebello, T. *J. Gene Med.* **2013**, *15*, 78−82.
(5) Townsend, M. H.; Shrestha, G.; Robison, R. A.; O'Neill, K. L. *J. Exp. Clin. Cancer Res.* **2018**, *37*, No. 163.
(6) Wang, J.; Hu, Y.; Huang, H. *Stem Cell Invest.* **2018**, *5*, No. 44.
(7) Simon, B.; Harrer, D. C.; Thirion, C.; Schuler-Thurner, B.; Schuler, G.; Uslu, U. *J. Immunol. Methods* **2019**, *472*, 55−64.
(8) Segura, M. M.; Garnier, A.; Durocher, Y.; Coelho, H.; Kamen, A. *Biotechnol. Bioeng.* **2007**, *98*, 789−799.
(9) Tiscornia, G.; Singer, O.; Verma, I. M. *Nat. Protoc.* **2006**, *1*, 241−245.
(10) Geraerts, M.; Willems, S.; Baekelandt, V.; Debyser, Z.; Gijsbers, R. *BMC Biotechnol.* **2006**, *6*, No. 34.
(11) Merten, O. W.; Charrier, S.; Laroudie, N.; Fauchille, S.; Dugué, C.; Jenny, C.; Audit, M.; Zanta-Boussif, M. A.; Chautard, H.; Radrizzani, M.; Vallanti, G.; Naldini, L.; Noguiez-Hellin, P.; Galy, A. *Hum. Gene Ther.* **2011**, *22*, 343−56.
(12) Kutner, R. H.; Puthli, S.; Marino, M. P.; Reiser, J. *BMC Biotechnol.* **2009**, *9*, No. 10.
(13) Tran, R.; Myers, D. R.; Denning, G.; Shields, J. E.; Lytle, A. M.; Alrowais, H.; Qiu, Y.; Sakurai, Y.; Li, W. C.; Brand, O.; Le Doux, J. M.; Spencer, H. T.; Doering, C. B.; Lam, W. A. *Mol. Ther.* **2017**, *25*, 2372−2382.
(14) Moore, N.; Chevillet, J. R.; Healey, L. J.; McBrine, C.; Doty, D.; Santos, J.; Teece, B.; Truslow, J.; Mott, V.; Hsi, P.; Tandon, V.; Borenstein, J. T.; Balestrini, J.; Kotz, K. *Sci. Rep.* **2019**, *9*, No. 15101.
(15) Cimetta, E.; Franzoso, M.; Trevisan, M.; Serena, E.; Zambon, A.; Giulitti, S.; Barzon, L.; Elvassore, N. *Biomicrofluidics* **2012**, *6*, No. 024127.
(16) Silva, P. N.; Atto, Z.; Regeenes, R.; Tufa, U.; Chen, Y. Y.; Chan, W. C. W.; Volchuk, A.; Kilkenny, D. M.; Rocheleau, J. V. *Lab Chip* **2016**, *16*, 2921−2934.
(17) Chuck, A. S.; Clarke, M. F.; Palsson, B. O. *Hum. Gene Ther.* **1996**, *7*, 1527−34.
(18) Choi, K.; Ng, A. H. C.; Fobel, R.; Wheeler, A. R. *Annu. Rev. Anal. Chem.* **2012**, *5*, 413−440.
(19) Barbulovic-Nad, I.; Yang, H.; Park, P. S.; Wheeler, A. R. *Lab Chip* **2008**, *8*, 519−526.
(20) Barbulovic-Nad, I.; Au, S. H.; Wheeler, A. R. *Lab Chip* **2010**, *10*, 1536−1542.
(21) Sinha, H.; Quach, A. B. V.; Vo, P. Q. N.; Shih, S. C. C. *Lab Chip* **2018**, *18*, 2300−2312.
(22) Eydelnant, I. A.; Uddayasankar, U.; Li, B. B.; Liao, M. W.; Wheeler, A. R. *Lab Chip* **2012**, *12*, 750−757.
(23) Srigunapalan, S.; Eydelnant, I. A.; Simmons, C. A.; Wheeler, A. R. *Lab Chip* **2012**, *12*, 369−375.
(24) Zhai, J.; Li, H.; Wong, A. H.-H.; Dong, C.; Yi, S.; Jia, Y.; Mak, P.-I.; Deng, C.-X.; Martins, R. P. *Microsyst. Nanoeng.* **2020**, *6*, No. 6.
(25) Lamanna, J.; Scott, E. Y.; Edwards, H. S.; Chamberlain, M. D.; Dryden, M. D. M.; Peng, J.; Mair, B.; Lee, A.; Chan, C.; Sklavounos, A. A.; Heffernan, A.; Abbas, F.; Lam, C.; Olson, M. E.; Moffat, J.; Wheeler, A. R. *Nat. Commun.* **2020**, *11*, No. 5632.
(26) Gill, K. P.; Denham, M. *Curr. Protoc. Mol. Biol.* **2020**, *133*, No. e125.
(27) Husser, M. C.; Vo, P. Q. N.; Sinha, H.; Ahmadi, F.; Shih, S. C. C. *ACS Synth. Biol.* **2018**, *7*, 933−944.
(28) Leclerc, L. M. Y.; Soffer, G.; Kwan, D. H.; Shih, S. C. C. *Biomicrofluidics* **2019**, *13*, No. 034106.
(29) Anderson, S.; Hadwen, B.; Brown, C. *Lab Chip* **2021**, *21*, 962−975.
(30) Saunderson, E. A.; Stepper, P.; Gomm, J. J.; Hoa, L.; Morgan, A.; Allen, M. D.; Jones, J. L.; Gribben, J. G.; Jurkowski, T. P.; Ficz, G. *Nat. Commun.* **2017**, *8*, No. 1450.
(31) Vijayraghavan, S.; Kantor, B. *J. Vis. Exp.* **2017**, No. 56915.
(32) Merten, O. W.; Hebben, M.; Bovolenta, C. *Mol. Ther.–Methods Clin. Dev.* **2016**, *3*, No. 16017.
(33) Cao, F.; Xie, X.; Gollan, T.; Zhao, L.; Narsinh, K.; Lee, R. J.; Wu, J. C. *Mol. Imaging Biol.* **2010**, *12*, 15−24.
(34) Aznan, A. N.; Abdul Karim, N.; Wan Ngah, W. Z.; Jubri, Z. *Oncol. Lett.* **2018**, *16*, 73−82.
(35) Gouvarchin Ghaleh, H. E.; Bolandian, M.; Dorostkar, R.; Jafari, A.; Pour, M. F. *Biomed. Pharmacother.* **2020**, *128*, No. 110276.
(36) Brown, L. Y.; Dong, W.; Kantor, B. *STAR Protoc.* **2020**, *1*, No. 100152.

(37) McCarron, A.; Donnelley, M.; Parsons, D. *Cell Gene Ther. Insights* **2017**, *3*, 719−729.
(38) Manceur, A. P.; Kim, H.; Misic, V.; Andreev, N.; Dorion-Thibaudeau, J.; Lanthier, S.; Bernier, A.; Tremblay, S.; Gélinas, A.-M.; Broussau, S.; Gilbert, R.; Ansorge, S. *Hum. Gene Ther. Methods* **2017**, *28*, 330−339.
(39) Sinn, P. L.; Sauter, S. L.; McCray, P. B. *Gene Ther.* **2005**, *12*, 1089−1098.
(40) Counsell, J. R.; Asgarian, Z.; Meng, J.; Ferrer, V.; Vink, C. A.; Howe, S. J.; Waddington, S. N.; Thrasher, A. J.; Muntoni, F.; Morgan, J. E.; Danos, O. *Sci. Rep.* **2017**, *7*, No. 44775.
(41) Wotherspoon, S.; Dolnikov, A.; Symonds, G.; Nordon, R. *J. Virol.* **2004**, *78*, 5097−102.
(42) Pirona, A. C.; Oktriani, R.; Boettcher, M.; Hoheisel, J. D. *Biol. Methods Protoc.* **2020**, *5*, No. bpaa005.
(43) Hines, W. C.; Yaswen, P.; Bissell, M. J. *Nat. Commun.* **2015**, *6*, No. 6927.
(44) Kumar, M.; Keller, B.; Makalou, N.; Sutton, R. E. *Hum. Gene Ther.* **2001**, *12*, 1893−1905.
(45) Ellis, B. L.; Hirsch, M. L.; Barker, J. C.; Connelly, J. P.; Steininger, R. J.; Porteus, M. H. *Virol. J.* **2013**, *10*, No. 74.
(46) Klein, R. L.; Dayton, R. D.; Tatom, J. B.; Henderson, K. M.; Henning, P. P. *Mol. Ther.* **2008**, *16*, 89−96.
(47) Hirsch, M. L.; Fagan, B. M.; Dumitru, R.; Bower, J. J.; Yadav, S.; Porteus, M. H.; Pevny, L. H.; Samulski, R. J. *PLoS One* **2011**, *6*, No. e27520.
(48) Traboulsi, T.; El Ezzy, M.; Gleason, J. L.; Mader, S. *J. Mol. Endocrinol.* **2017**, *58*, R15−R31.
(49) Xiao, T.; Li, W.; Wang, X.; Xu, H.; Yang, J.; Wu, Q.; Huang, Y.; Geradts, J.; Jiang, P.; Fei, T.; Chi, D.; Zang, C.; Liao, Q.; Rennhack, J.; Andrechek, E.; Li, N.; Detre, S.; Dowsett, M.; Jeselsohn, R. M.; Liu, X. S.; Brown, M. *Proc. Natl. Acad. Sci. U.S.A.* **2018**, *115*, 7869−7878.
(50) Taylor, S. C.; Nadeau, K.; Abbasi, M.; Lachance, C.; Nguyen, M.; Fenrich, J. *Trends Biotechnol.* **2019**, *37*, 761−774.
(51) Li, H.; Yang, Y.; Hong, W.; Huang, M.; Wu, M.; Zhao, X. *Signal Transduction Targeted Ther.* **2020**, *5*, No. 1.
(52) Tian, X.; Gu, T.; Patel, S.; Bode, A. M.; Lee, M.-H.; Dong, Z. *npj Precis. Oncol.* **2019**, *3*, No. 8.
(53) Liu, B.; Saber, A.; Haisma, H. J. *Drug Discovery Today* **2019**, *24*, 955−970.
(54) Alimperti, S.; Lei, P.; Tian, J.; Andreadis, S. T. *Gene Ther.* **2012**, *19*, 1123−1132.
(55) Xu, X.; Gao, D.; Wang, P.; Chen, J.; Ruan, J.; Xu, J.; Xia, X. *Sci. Rep.* **2018**, *8*, No. 11649.
(56) Ran, F. A.; Hsu, P. D.; Wright, J.; Agarwala, V.; Scott, D. A.; Zhang, F. *Nat. Protoc.* **2013**, *8*, 2281−2308.
(57) Samlali, K.; Ahmadi, F.; Quach, A. B. V.; Soffer, G.; Shih, S. C. C. *Small* **2020**, *16*, No. 2002400.
(58) Li, X.; Aghaamoo, M.; Liu, S.; Lee, D.-H.; Lee, A. P. *Small* **2018**, *14*, No. 1802055.
(59) Han, X.; Liu, Z.; Ma, Y.; Zhang, K.; Qin, L. *Adv. Biosyst.* **2017**, *1*, No. 1600007.
(60) Han, X.; Liu, Z.; Zhao, L.; Wang, F.; Yu, Y.; Yang, J.; Chen, R.; Qin, L. *Angew. Chem., Int. Ed.* **2016**, *55*, 8561−8565.
(61) Xing, Y.; Liu, Y.; Chen, R.; Li, Y.; Zhang, C.; Jiang, Y.; Lu, Y.; Lin, B.; Chen, P.; Tian, R.; Liu, X.; Cheng, X. *Lab Chip* **2021**, *21*, 1886−1896.

https://doi.org/10.1021/acs.analchem.1c05227
Anal. Chem. 2022, 94, 4039−4047